

SEE Test Report V.2  
Single event effects testing of the Vishay  
Si7431DP p-type Power MOSFET

Jean-Marie Lauenstein, NASA/GSFC  
Dakai Chen, Anthony Phan, Timothy Irwin, and Hak Kim, MEI Technologies

Test Date: 23 January 2011, 28 March 2011

Report Date: 8 July 2011  
V.2: 22 July 2011

### I. Introduction and Summary of Test Results

This study was being undertaken to determine the single event effect susceptibility of the Si7431DP power MOSFET. This test was conducted at the Lawrence Berkeley 88" Cyclotron Facility (LBNL). Its purpose is to evaluate this device as a candidate for use in NASA flight projects, as well as to examine the heavy-ion response of a p-type trenchFET power device structure.

All failures during these tests were due to single-event gate rupture (SEGR). All tests were conducted at ambient temperature in vacuum at either 0°, 45°, or 60° off-normal beam incidence. A summary of the minimum last pass/first fail drain-source voltage (V<sub>ds</sub>) for a given gate-source voltage bias (V<sub>gs</sub>) and angle is provided in Table 1 below as a function of the ion species, as well as energy, range, and LET at the surface of the device under test (DUT). The total number of devices tested under each beam and bias condition is shown in the final column. The normal-incident data are plotted in Figure 1 and the angular data in Figure 2.

Table 1: Summary of heavy-ion test results. All failures are due to SEGR.

Ion Specie	Surface-Incident Energy (MeV)	Range (μm)	Surface-Incident LET (MeV·cm <sup>2</sup> /mg)	Angle (deg)	V <sub>gs</sub> (V)	Maximum Last Passing V <sub>ds</sub> (V)	Maximum V <sub>ds</sub> at Failure (V)	# of Devices Tested					
Kr	1230	165.4	25	0	0	-200	--	3					
					5	-200	--	2					
					10	-120	-130	1					
				45	0	-200	--	2					
					60	0	-200	--	2				
						5	-200	--	1				
				60	10	-200	--	2					
					Ag	1039	90	48.15	0	0	-150	-155	3
										5	-90	-100	2
10	-30	-40	2										

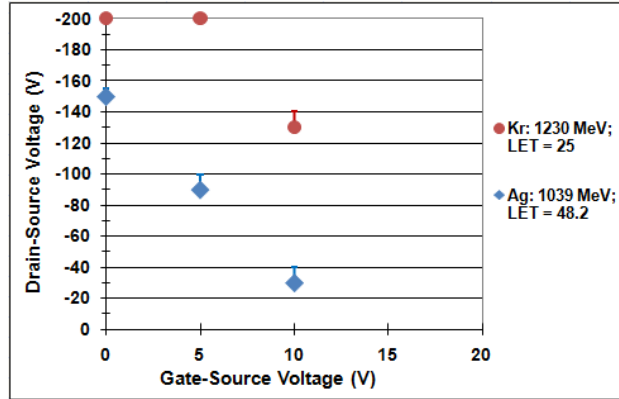


Figure 1. SEE response curve for the Si7431DP.

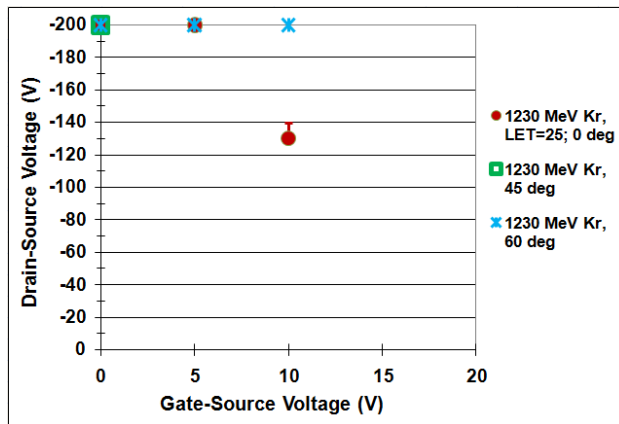


Figure 2. Effect of angle of incidence on the SEE response curve defined under krypton irradiation. These data indicate normal incidence is worst-case for the Si7431DP.

## II. Devices Tested

The sample size for the testing was 30 pieces and one control. The part is manufactured by Vishay Intertechnology, and introduced in 2005 as part of their TrenchFET® technology.

The device is a commercial 3.8 A, 200 V p-channel trench power MOSFET, part #Si7431DP. The samples to be tested were provided by Vishay in January, 2011 in PowerPAK SO-8 surface-mount plastic packaging. Five samples were decapsulated by Vishay prior to shipment; the additional 17 samples were decapsulated with fuming nitric acid by Timothy Irwin, MEI Technologies. The pieces were visually inspected and electrically characterized on-site by Anthony Phan, MEI Technologies. The LDCs for the parts tested are ZZ W54B and AB W08B (2 samples only). The die measures approximately 0.371 cm x 0.349 cm for a total area of 0.130 cm<sup>2</sup>. The die features a closed-cell topology; the trenches therefore have no single orientation with respect to the die.

### III. Test Facility

- Facility:** Lawrence Berkeley National Laboratory 88" Cyclotron Facility, 10 MeV/amu and 16 MeV/amu tune.
- Flux:**  $1.5 \times 10^4$  particles/cm<sup>2</sup>/s to  $3.7 \times 10^4$  particles/cm<sup>2</sup>/s.
- Fluence:** All tests were run to the lesser of  $3 \times 10^5$  ions/cm<sup>2</sup> or until destructive events occur.
- Ion species:** Kr and Ag. The table below shows the surface-incident beam properties (Tests were performed in vacuum).

Table 2. Ion beam properties.

Ion:	Beam Tune (MeV/u)	Surface Energy (MeV)	Surface LET (MeV•cm <sup>2</sup> /mg)	Range (μm)	Angle of Incidence (Degrees)
<sup>78</sup> Kr	16	1230	25	165.4	0, 45, 60
<sup>107</sup> Ag	10	1039	48.15	90	0

### IV. Test Setup

The test circuit, as shown in Figure 4, for the power MOSFET contains a Keithley 2400 source meter to provide the gate voltage (set to 0 V, 5 V, or 10 V during irradiation) while measuring the gate current. A filter is placed at the gate node of each device under test (DUT) to dampen noise at the gate. A second Keithley 2400 source meter provides the appropriate V<sub>ds</sub> while measuring the drain current. Gate current is limited to 1 mA, and drain current limited to 100 mA, and recorded via GPIB card to a desktop computer at 150 ms intervals.

A Tektronix P6139A 10 MΩ, 500 MHz probe across the 1 Ω drain sense resistor feeds into a digital oscilloscope that is set to trigger on current transients of a predetermined size, saving them to file. If desirable for error mode analysis, a current limiting resistor may be jumpered into series with the drain to protect the DUT from destructive SEB. Nine DUTs can be mounted on the test board and individually accessed via a switch box within the control room. The terminals of the devices not under test are then shorted to ground. Testing was conducted in vacuum with the DUT centered within the beam diameter. Ion exposures were conducted at either a 0°, 45°, or 60° angle of incidence to the DUT. The device has a closed-cell topology, so that there is no specific trench orientation with respect to the die.

The test setup is controlled via custom LabView codes written by Hak Kim for this test. One program controls the source measuring units (SMUs), gate current limit, oscilloscope monitoring and transient capture, and gate and drain current sampling and recording. The second LabView code is designed to perform a parametric analysis of each DUT prior to irradiation and following each beam run, recording I<sub>gs</sub> as a function of V<sub>gs</sub> (gate stress test to test the integrity of the gate dielectric), I<sub>ds</sub> as a function of V<sub>gs</sub> at various fixed V<sub>ds</sub> values for evaluation of total ionizing dose effects, gate threshold voltage (V<sub>th</sub>), drain-source breakdown voltage (BV<sub>dss</sub>), and zero gate voltage drain current (I<sub>dss</sub>).

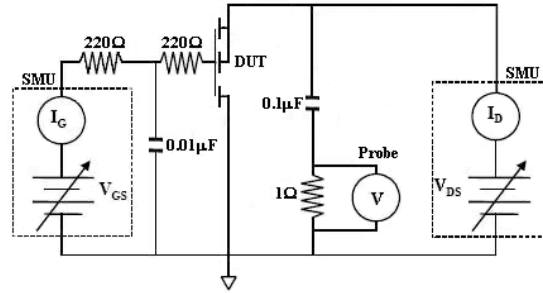


Figure 3. Test setup for the Si7431DP power MOSFET.

Table 3. Test equipment.

Node	Make/model	s/n
Gate	Keithley 2400 source meter	1173709
Drain	Keithley 2400 source meter Tektronix DPO4054 Tektronix P6139A GW Instek PST-3202 Programmable power supply	1247482 B020036 E1211978
Other	2 Lenovo IBM ThinkCentre desktop computers Power Conditioner Switchbox (custom design)	

## V. Test Results

Tests were performed at the Berkeley Accelerator Space Effects Facility 88" Cyclotron at Lawrence Berkeley National Laboratory (LBNL) on January 23-24, 2011 by Dakai Chen and Anthony Phan; additional tests were performed at LBNL on March 28, 2011 by Hak Kim and Anthony Phan. Two monoenergetic ion beams (1230 MeV krypton and 1039 MeV silver) were used; all tests were conducted in vacuum with the beam at various angles of incidence to the DUT. Following each run, a post-irradiation gate stress (PIGS) test was performed in which the gate current was measured while the gate voltage was swept from 0V to -20V, then from 0V to 20V, at 0Vds. Each voltage step at a 2-volt increment was held for 500 ms to allow settling prior to the current reading. In addition, Id-Vgs curves were swept at Vds values of -0.05 V, and Idss measured, to check for ionizing dose effects and device integrity. Failure was defined as the gate current exceeding the vendor specification of 100 nA during the beam run or during the PIGS test, and/or a sudden, sustained increase in the drain current during the beam run. The Idss measurements taken while the test board was in the vacuum chamber show elevated leakage current. This current leakage was determined to come from the patch panel on the vacuum chamber (ribbon connector interface between the inside and outside of the vacuum chamber). Bypassing this connector interface using a free-standing ribbon connector (with the chamber necessarily open) to couple the wiring going to the chamber with that going to the test board eliminated this leakage current. No cross-talk between connector pins in the patch panel could be detected, suggesting that the pins were individually isolated; the source of the leakage could not be determined. The Idss values recorded during testing should therefore be assessed accordingly by comparing them with the pre-rad value measured with the device in the chamber (indicated on the test results spreadsheet in Appendix C). Table I in Section I summarizes the heavy-ion test results for each bias and beam condition, and Figure 1 in that section plots the results. Table 4 below lists the last pass/first fail bias for the individual devices tested. Device

electrical specifications are provided in Appendix A, and pretest electrical characterization results are in Appendix B. Complete results are in Appendix C, with PIGS test results provided in Appendix D and example striptape current measurements in Appendix E.

The primary failure mode for this device is SEGR. Failures under 0 Vgs and 5 Vgs bias occurred during the PIGS test, suggesting latent damage to the gate (SEGR). Under 10 Vgs bias, SEGR occurred during the beam run. The device demonstrated reduced sensitivity to failure when the ion beam incidence was at an angle to the device surface. A study of n-type trenchFETs revealed increasing SEGR sensitivity with increasing angle<sup>1</sup>; for these devices, the gate oxide was thicker at the bottom of the trench than along the trench walls, such that ruptures likely occurred more easily in the wall of the trench oxide.

Table 4. Summary of individual sample results as a function of bias conditions and beam properties.

Ion Specie	Surface-Incident Energy	Range	Surface-Incident LET	Angle	Vgs	Maximum Last Passing Vds	Maximum Vds at Failure			
	(MeV)	(um)	(MeV·cm <sup>2</sup> /mg)	(deg)	(V)	(V)	(V)			
Kr	1230	165	25		0	-200	--			
						-200	--			
						-200	--			
						5	-200	--		
							-200	--		
						10	--	-200		
							--	-180		
							--	-150		
							-120	-140		
							-120	-125		
						--	-110			
						45	0	-200	--	
							-200	--		
						60	0	-200	--	
							-200	--		
							5	-200	--	
						10	-200	--		
							-200	--		
Ag	1039	90	48.15			0	-165	-170		
							--	-170		
							--	-170		
							--	-170		
							-150	-155		
							-160	-165		
						--	-160			
						5	--	-130		
							--	-100		
							-100*	-110		
						10	-30	-40		

\* last clean run at -95V

<sup>1</sup> Liu, S., *et al.*, "Vulnerable Trench Power MOSFETs under Heavy Ion Irradiation," presented at IEEE Nuclear Space and Radiation Effects Conference, Tuscan, AZ, July 2010.

			-35	-40
--	--	--	-----	-----

**Appendix A**

Table A1. Si7431DP vendor-specified electrical parameters (partial list).

<b>Parameter</b>	<b>Condition</b>	<b>MIN</b>	<b>MAX</b>	<b>Units</b>
Gate Threshold Voltage (VGSth)	$V_{ds} = V_{gs}$ , $I_d = -250 \mu A$	-2.0	-4.0	V
Zero Gate Voltage Drain Current (Idss)	$V_{ds} = -200 V$ , $V_{gs} = 0 V$		-1	$\mu A$
Drain-Source Breakdown Voltage (BVdss)	<i>(not specified)</i>			
Gate-Source Leakage Current (I <sub>gss</sub> )	$V_{gs} = +/- 20 V$ , $V_{ds} = 0 V$		+/-100	nA
Static Drain-Source Resistance (R <sub>ds_on</sub> )	$V_{gs} = -10 V$ , $I_d = -3.8 A$ $V_{gs} = -6 V$ , $I_d = -3.6 A$		174 180	m $\Omega$
Forward Voltage (Vsd)	$I_s = -4.2 A$ , $V_{gs} = 0V$		-1.2	V

## Appendix B

Table B1. Pretest electrical characterization.

Part SN	LDC	Vth (Volts)	BVdss (Volts)	Idss (nA)	Igss - (A)	Igss + (A)
1	ZZ-W54B	-3.19	< -200	-9.158	-1.38E-09	1.25E-09
3	ZZ-W54B	-3.14	< -200	-52.33	-1.49E-09	1.31E-09
4	ZZ-W54B	-3.08	< -200	-18.19	-1.374E-09	1.29E-09
5	ZZ-W54B	-3.09	< -200	-17.61	-1.4E-09	1.32E-09
6	ZZ-W54B	-3.13	< -200	-14.15	-1.33E-09	1.21E-09
7	ZZ-W54B	-3.1	< -200	-26.6	-1.44E-09	1.33E-09
8	ZZ-W54B	-3.11	< -200	-20.86	-1.341E-09	1.281E-09
9	ZZ-W54B	-3.03	< -200	-19.74	-1.49E-09	1.33E-09
10	ZZ-W54B	-3.11	< -200	-23.3	-1.32E-09	1.22E-09
11	ZZ-W54B	-3.09	< -200	-12.31	-1.35E-09	1.35E-09
12	ZZ-W54B	-3.13	< -200	-14.62	-1.38E-09	1.4E-09
13	ZZ-W54B	-3.12	< -200	-12.78	-1.34E-09	1.34E-09
14	ZZ-W54B	-3.11	< -200	-4.172	-1.52E-09	1.36E-09
15	ZZ-W54B	-2.9	< -200	-1.45	-1.33E-09	1.29E-09
16	ZZ-W54B	-3.15	< -200	-9.447	-1.56E-09	1.36E-09
17	ZZ-W54B	-3.21	< -200	-20.28	-1.37E-09	1.28E-09
18	ZZ-W54B	-3.14	< -200	-65	-1.58E-09	1.42E-09
19	ZZ-W54B	-2.95	< -200	-58.78	-1.35E-09	1.32E-09
20	ZZ-W54B	-2.97	< -200	-58.83	-1.35E-09	1.27E-09
21	ZZ-W54B	-3.1	< -200	-57.3	-1.53E-09	1.34E-09
22	ZZ-W54B	-3.09	< -200	-59.96	-1.39E-09	1.32E-09
23	ZZ-W54B	-2.9	< -200	-9.455	-1.37E-09	1.34E-09
41	AB-W08B	-3.22	-221	-48.28	-1.30E-09	1.29E-09
42	AB-W08B	-3.13	-206	-180.16	-1.45E-09	1.33E-09

## Appendix C (next page)

Table C1. Raw test data. LET, energy, and range are at the die surface. Note that Idss measurements reflect occasional high leakage current from vacuum chamber connection; pretest measurements in Appendix B were made outside of chamber.



Run Date	Time	Run #	Ion	LET MeV.cm2/mg	Energy MeV/amu	Energy MeV	Range μm	Ave. Flux #/cm2/sec	Eff. Fluence #/cm2	S/N	socket #	Angle deg	VGS V	VDS V	Vth V	Idss μA	Pass/Fail Blank=Pass	Comments
1/23/11	11:49	1	Ag	48.15	10	1039	90	3.70E+04	3.15E+05	1	1	0	0	-160	-3.18	NA		
		2	Ag	48.15	10	1039	90	3.54E+04	3.22E+05	1	1	0	0	-165	-3.18	NA		
		3	Ag	48.15	10	1039	90	3.62E+04	3.20E+05	1	1	0	0	-170	NA	NA	F	Failed PIGS
		4	Ag	48.15	10	1039	90	3.56E+04	3.19E+05	3	3	0	0	-170	NA	NA		run nulified.
		5	Ag	48.15	10	1039	90	3.40E+04	2.42E+05	3	3	0	0	-170	NA	NA	F	Failed PIGS
		6	Ag	48.15	10	1039	90	3.42E+04	3.25E+05	4	4	0	0	-170	-3.08	>2		Increased compliance to 2uA for Idss test due to noise level; prerad Idss ~600nA
		7	Ag	48.15	10	1039	90	3.48E+04	3.20E+05	4	4	0	0	-170	NA	>2	F	Failed PIGS.
		8	Ag	48.15	10	1039	90	3.34E+04	3.23E+05	5	5	0	0	-170	NA	>2	F	Failed PIGS
		9	Ag	48.15	10	1039	90	2.64E+04	3.18E+05	6	6	0	0	-150	-3.13	>2		Idss~900nA prerad
		10	Ag	48.15	10	1039	90	3.29E+04	3.09E+05	6	6	0	0	-155	NA	>2	F	Failed PIGS
		11	Ag	48.15	10	1039	90	3.36E+04	3.16E+05	7	7	0	0	-155	-3.10	2.33		Idss breakdown test set compliance to 3 uA. Idss~2.8uA prerad @ 166V
		12	Ag	48.15	10	1039	90	3.34E+04	3.24E+05	7	7	0	0	-160	-3.10	2.36		
		13	Ag	48.15	10	1039	90	3.23E+04	3.21E+05	7	7	0	0	-165	NA	>3uA @ 0V	F	failed PIGS
		14	Ag	48.15	10	1039	90	NA	NA	8	8	0	0	-160	NA	NA	NA	no beam, run nulified
		15	Ag	48.15	10	1039	90	3.17E+04	3.25E+05	8	8	0	0	-160	-3.11	> 3uA @ 0V	F	failed PIGS; prerad Idss~1.63uA @ 200V
		16	Ag	48.15	10	1039	90	3.00E+04	3.12E+05	9	9	0	0	-150	-3.11	0.589		prerad Idss~500nA @ 200V
		17	Ag	48.15	10	1039	90	2.99E+04	3.12E+05	9	9	5	5	-150	-3.03	> 3uA @ 36V	F	failed PIGS; prerad Idss~600nA @ 200V
	14:34	18	Ag	48.15	10	1039	90	2.76E+04	3.14E+05	10	1	0	5	-130	-3.11	0.035	F	prerad Idss~34nA @ 200V; failed PIGS reset Idss compliance to 1uA. prerad Idss~34nA @ 200V; failed PIGS
		19	Ag	48.15	10	1039	90	2.72E+04	3.15E+05	11	2	0	5	-100	-3.09	-1uA @ 62V	F	
		20	Ag	48.15	10	1039	90	2.56E+04	3.20E+05	12	3	0	5	-50	-3.12	0.321		prerad Idss~368nA @ 200V
		21	Ag	48.15	10	1039	90	2.50E+04	3.10E+05	12	3	0	5	-60	-3.12	0.354		
		22	Ag	48.15	10	1039	90	2.52E+04	3.08E+05	12	3	0	5	-70	NA	0.342		
		23	Ag	48.15	10	1039	90	2.62E+04	3.17E+05	12	3	0	5	-80	NA	0.364		
		24	Ag	48.15	10	1039	90	2.48E+04	3.12E+05	12	3	0	5	-90	NA	0.378		
		25	Ag	48.15	10	1039	90	2.43E+04	3.10E+05	12	3	0	5	-100	-3.12	0.374		postrad: Ig increased -order of mag
		26	Ag	48.15	10	1039	90	2.45E+04	3.11E+05	12	3	0	5	-110	-3.12	> 1uA @ 26V	F	failed PIGS
		27	Ag	48.15	10	1039	90	2.39E+04	3.09E+05	13	4	0	5	-90	-3.12	0.373		prerad Idss~399 nA @ 200V
	15:46	28	Ag	48.15	10	1039	90	1.96E+04	3.15E+05	13	4	0	5	-100	-3.12	0.367	F	failed PIGS
		39	Ag	48.15	10	1039	90	2.22E+04	3.08E+05	14	5	0	10	-30	-3.11	0.525		prerad: Idss~500nA@200V, Vth=-3.1V
		40	Ag	48.15	10	1039	90	2.27E+04	3.14E+05	14	5	0	10	-40	-3.10	>3uA @ 3V	F	Failed during run
		41	Ag	48.15	10	1039	90	2.29E+04	3.09E+05	15	6	0	10	-30	-2.88			Vth=-2.88V.
		42	Ag	48.15	10	1039	90	2.26E+04	3.15E+05	15	6	0	10	-35	-2.88			
	19:22	43	Ag	48.15	10	1039	90	2.25E+04	3.14E+05	15	6	0	10	-40	-2.88		F	End runs with 10 MeV cocktail, switching to 16 MeV beam
		49	Kr	25	16	1230	165	1.92E+04	3.11E+05	20	1	0	0	-140	-2.97	1.12		prerad: Idss~1.2uA@200V, Vth=-2.97V.
		50	Kr	25	16	1230	165	1.85E+04	3.05E+05	20	1	0	0	-150				
		51	Kr	25	16	1230	165	1.91E+04	6.28E+04	20	1	0	0	-160				
		52	Kr	25	16	1230	165	2.09E+04	6.28E+04	20	1	0	0	-160				
		53	Kr	25	16	1230	165	1.83E+04	3.09E+05	20	1	0	0	-170	-2.97	1.15		
		54	Kr	25	16	1230	165	1.85E+04	3.14E+05	20	1	0	0	-180				
		55	Kr	25	16	1230	165	1.87E+04	3.11E+05	20	1	0	0	-190	-2.97	1.19		
		56	Kr	25	16	1230	165	1.84E+04	3.06E+05	20	1	0	0	-200	-2.97	1.17		
		57	Kr	25	16	1230	165	1.78E+04	3.09E+05	21	2	0	0	-180	-3.10	0.384		prerad: Idss~397nA@200V, Vth=-3.1
		58	Kr	25	16	1230	165	1.79E+04	3.08E+05	21	2	0	0	-190				
		59	Kr	25	16	1230	165	1.79E+04	3.07E+05	21	2	0	0	-200	-3.09	0.397		
		60	Kr	25	16	1230	165	1.76E+04	3.08E+05	23	6	0	0	-160	-2.90	1.08		prerad: Idss~1.05uA@200V, Vth=-2.9V
		61	Kr	25	16	1230	165	1.82E+04	3.09E+05	23	6	0	0	-170	-2.90	1.23		
		62	Kr	25	16	1230	165	1.68E+04	3.14E+05	23	6	0	0	-180				
		63	Kr	25	16	1230	165	1.67E+04	3.08E+05	23	6	0	0	-190				
		64	Kr	25	16	1230	165	1.75E+04	3.13E+05	23	6	0	0	-200	-2.90	1.02uA @ 175V		
		65	Kr	25	16	1230	165	1.81E+04	3.12E+05	16	7	45	0	-160				prerad: Idss~1.68uA@200V, Vth=-3.14V
		66	Kr	25	16	1230	165	1.73E+04	3.10E+05	16	7	45	0	-170	-3.14	1.59		
		67	Kr	25	16	1230	165	1.75E+04	3.11E+05	16	7	45	0	-180				
		68	Kr	25	16	1230	165	1.69E+04	3.06E+05	16	7	45	0	-190				
		69	Kr	25	16	1230	165	1.63E+04	3.07E+05	16	7	45	0	-200	-3.14	2.28		
		70	Kr	25	16	1230	165	1.58E+04	3.08E+05	17	8	45	0	-180	-3.21			Vth=-3.21V
		71	Kr	25	16	1230	165	1.60E+04	3.11E+05	17	8	45	0	-190	-3.21			
		72	Kr	25	16	1230	165	1.66E+04	3.10E+05	17	8	45	0	-200	-3.21			
		73	Kr	25	16	1230	165	1.60E+04	3.05E+05	18	9	60	0	-170		0.669		prerad: Idss~689nA@200V, Vth=-3.14
		74	Kr	25	16	1230	165	1.61E+04	3.06E+05	18	9	60	0	-180		0.747		
		75	Kr	25	16	1230	165	1.67E+04	3.09E+05	18	9	60	0	-190		0.719		
		76	Kr	25	16	1230	165	1.67E+04	3.12E+05	18	9	60	0	-200	-3.14	0.688		
		77	Kr	25	16	1230	165	1.60E+04	3.07E+05	22	5	60	0	-200	-3.09			
		78	Kr	25	16	1230	165	1.60E+04	3.09E+05	18	9	0	5	-170		0.446		
		79	Kr	25	16	1230	165	1.58E+04	3.09E+05	18	9	0	5	-180		0.549		
		80	Kr	25	16	1230	165	1.60E+04	3.08E+05	18	9	0	5	-190				
		81	Kr	25	16	1230	165	1.57E+04	3.07E+05	18	9	0	5	-200	-3.14	0.488		
		82	Kr	25	16	1230	165	1.57E+04	3.05E+05	17	8	0	5	-200	-3.21			
		83	Kr	25	16	1230	165	1.56E+04	3.07E+05	17	8	60	5	-200				
		84	Kr	25	16	1230	165	1.52E+04	3.07E+05	17	8	60	10	-200	-3.21			
		85	Kr	25	16	1230	165	1.53E+04	3.10E+05	21	2	60	10	-200	-3.09			Idss increased since last run
		86	Kr	25	16	1230	165	1.55E+04	3.02E+05	21	2	0	10	-200	-3.09		F	failed on run: Ig continued to increase after beam shuttered
		87	Kr	25	16	1230	165	1.46E+04	2.62E+05	17	8	0	10	-180				

Appendix D

Table D1. Post-irradiation gate stress (PIGS) test. Table contains PIGS test following the last passing run and first failing run for each DUT.

Run # DUT S/N	2 1	3 1	pre-5 3	5 3	6 4	7 4	pre-8 5	8 5	9 6	10 6
Date	1/23/2011	1/23/2011	1/23/2011	1/23/2011	1/23/2011	1/23/2011	1/23/2011	1/23/2011	1/23/2011	1/23/2011
Vgs (V):	Igs (A):									
0	-6.35E-10	-5.41E-10	-8.07E-10	-5.59E-10	-3.30E-10	-2.44E-10	-3.21E-10	-2.43E-10	-3.33E-10	-3.21E-10
-2	-9.46E-10	-8.71E-10	-1.34E-09	-7.34E-10	-5.87E-10	-9.91E-10	-5.15E-10	-3.49E-10	-3.96E-10	-6.67E-10
-4	-8.14E-10	-1.01E-09	-1.67E-09	-6.68E-10	-5.24E-10	-5.56E-09	-5.84E-10	-6.14E-10	-6.43E-10	-5.44E-10
-6	-1.42E-09	-8.13E-10	-1.27E-09	-1.03E-09	-7.02E-10	-3.22E-08	-7.06E-10	-8.11E-10	-5.59E-10	-8.02E-10
-8	-1.39E-09	-7.72E-10	-1.77E-09	-1.40E-09	-7.73E-10	-2.27E-07	-8.86E-10	-9.26E-10	-7.89E-10	-8.68E-10
-10	-1.15E-09	-1.50E-09	-1.40E-09	-1.57E-09	-1.09E-09	-4.37E-06	-9.99E-10	-1.14E-09	-9.84E-10	-1.34E-09
-12	-1.48E-09	-2.00E-09	-1.52E-09	-2.29E-09	-1.32E-09	-6.30E-05	-1.12E-09	-1.44E-09	-9.42E-10	-2.05E-09
-14	-1.66E-09	-3.79E-09	-1.77E-09	-3.39E-09	-1.44E-09	-4.05E-04	-1.19E-09	-2.24E-09	-1.30E-09	-3.63E-09
-16	-1.61E-09	-8.42E-09	-2.21E-09	-6.86E-09	-2.14E-09	-1.00E-03	-1.40E-09	-4.35E-09	-1.35E-09	-1.25E-08
-18	-1.85E-09	-2.11E-08	-2.00E-09	-2.14E-08	-3.29E-09	-1.00E-03	-1.33E-09	-9.74E-09	-1.93E-09	-2.71E-04
-20	-1.97E-09	-5.75E-04	-2.24E-09	-4.42E-04	-7.20E-09	-1.00E-03	-1.69E-09	-5.69E-04	-2.74E-09	-1.00E-03
2	6.36E-10	1.32E-06	-5.52E-11	6.71E-09	8.36E-10	6.99E-09	7.97E-10	4.71E-07	1.02E-09	8.22E-08
4	5.27E-10	4.86E-05	2.13E-10	2.22E-07	7.37E-10	1.52E-07	6.28E-10	4.44E-05	7.42E-10	5.43E-06
6	3.29E-10	2.12E-04	-5.02E-12	3.80E-05	4.05E-10	5.64E-05	6.66E-10	2.76E-04	7.10E-10	4.13E-04
8	6.16E-10	5.09E-04	8.97E-11	8.52E-05	5.18E-10	8.74E-04	6.50E-10	5.73E-04	7.21E-10	1.00E-03
10	3.95E-10	1.00E-03	3.32E-10	1.00E-03	7.45E-10	1.00E-03	7.65E-10	1.00E-03	7.38E-10	1.00E-03
12	4.87E-10	1.00E-03	1.11E-10	1.00E-03	9.71E-10	1.00E-03	9.02E-10	1.00E-03	1.02E-09	1.00E-03
14	5.06E-10	1.00E-03	3.64E-10	1.00E-03	1.41E-09	1.00E-03	1.10E-09	1.00E-03	1.10E-09	1.00E-03
16	5.65E-10	1.00E-03	1.69E-10	1.00E-03	1.90E-09	1.00E-03	1.11E-09	1.00E-03	1.43E-09	1.00E-03
18	6.03E-10	1.00E-03	7.44E-10	1.00E-03	3.21E-09	1.00E-03	1.47E-09	1.00E-03	1.52E-09	1.00E-03
20	1.16E-09	1.00E-03	9.66E-10	1.00E-03	6.90E-09	1.00E-03	1.45E-09	1.00E-03	2.19E-09	1.00E-03

Run # DUT S/N	12 7	13 7	pre-15 8	15 8	16 9	17 9	pre-18 10	18 10	pre-19 11	19 11
Date	1/23/2011	1/23/2011	1/23/2011	1/23/2011	1/23/2011	1/23/2011	1/23/2011	1/23/2011	1/23/2011	1/23/2011
Vgs (V):	Igs (A):									
0	-4.14E-10	-2.68E-10	-8.55E-10	-6.47E-10	-1.65E-10	-8.76E-10	3.03E-11	-6.00E-10	-7.25E-11	-7.05E-10
-2	-4.37E-10	-4.67E-10	-9.09E-10	-8.19E-10	-4.69E-10	-7.40E-10	-2.38E-10	-5.94E-10	-2.67E-10	-7.56E-10
-4	-6.85E-10	-7.96E-10	-8.13E-10	-9.58E-10	-8.05E-10	-8.58E-10	-3.51E-10	-7.22E-10	-4.10E-10	-8.03E-10
-6	-5.77E-10	-8.55E-10	-1.02E-09	-1.34E-09	-7.03E-10	-1.07E-09	-5.19E-10	-7.95E-10	-5.11E-10	-9.85E-10
-8	-1.08E-09	-1.10E-09	-1.00E-09	-1.53E-09	-1.15E-09	-9.78E-10	-6.75E-10	-8.58E-10	-7.09E-10	-9.65E-10
-10	-1.28E-09	-1.50E-09	-1.38E-09	-1.58E-09	-9.95E-10	-1.23E-09	-7.91E-10	-9.89E-10	-9.52E-10	-1.14E-09
-12	-1.09E-09	-2.44E-09	-1.22E-09	-2.30E-09	-1.25E-09	-2.07E-09	-8.72E-10	-1.24E-09	-1.13E-09	-1.37E-09
-14	-1.50E-09	-4.61E-09	-1.48E-09	-4.36E-09	-1.26E-09	-3.66E-09	-1.05E-09	-1.73E-09	-1.26E-09	-1.57E-09
-16	-1.66E-09	-1.16E-08	-1.54E-09	-9.88E-09	-1.53E-09	-8.52E-09	-1.29E-09	-3.26E-09	-1.41E-09	-2.36E-09
-18	-1.34E-09	-3.24E-08	-1.84E-09	-2.48E-08	-1.57E-09	-2.64E-08	-1.29E-09	-6.42E-09	-1.51E-09	-4.59E-09
-20	-1.79E-09	-5.63E-04	-2.10E-09	-9.46E-04	-2.03E-09	-5.86E-04	-1.39E-09	-8.11E-04	-1.62E-09	-8.55E-04
2	1.18E-09	1.12E-08	5.09E-10	1.74E-07	7.77E-10	6.18E-07	9.42E-10	4.75E-09	1.06E-09	1.04E-08
4	7.31E-10	6.92E-06	2.23E-10	6.68E-06	7.36E-10	2.50E-05	7.86E-10	1.81E-07	8.00E-10	1.30E-06
6	6.86E-10	2.01E-04	8.51E-11	1.67E-04	5.22E-10	2.66E-04	9.05E-10	3.50E-05	9.26E-10	4.37E-04
8	7.13E-10	4.52E-04	1.77E-10	1.00E-03	5.13E-10	2.35E-04	8.38E-10	8.14E-04	9.71E-10	1.00E-03
10	9.37E-10	1.00E-03	5.94E-10	1.00E-03	6.94E-10	1.00E-03	8.90E-10	1.00E-03	1.07E-09	1.00E-03
12	9.37E-10	1.00E-03	6.18E-10	1.00E-03	6.89E-10	1.00E-03	9.55E-10	1.00E-03	1.14E-09	1.00E-03
14	9.74E-10	1.00E-03	9.85E-10	1.00E-03	7.62E-10	1.00E-03	1.07E-09	1.00E-03	1.26E-09	1.00E-03
16	1.29E-09	1.00E-03	7.12E-10	1.00E-03	1.03E-09	1.00E-03	1.13E-09	1.00E-03	1.36E-09	1.00E-03
18	1.23E-09	1.00E-03	6.54E-10	1.00E-03	9.82E-10	1.00E-03	1.45E-09	1.00E-03	1.40E-09	1.00E-03
20	1.68E-09	1.00E-03	8.99E-10	1.00E-03	1.32E-09	1.00E-03	1.49E-09	1.00E-03	1.58E-09	1.00E-03

Run # DUT S/N Date	24 12 1/23/2011	25 12 1/23/2011	26 12 1/23/2011	27 13 1/23/2011	28 13 1/23/2011	39 14 1/23/2011	40 14 1/23/2011	42 15 1/23/2011	43 15 1/23/2011	64 23 1/23/2011
Vgs (V):	Ids (A):									
-20	-2.51E-09	-1.30E-08	-1.00E-03	-1.64E-09	-1.00E-03	-1.80E-09	-1.00E-03	-1.83E-09	-1.00E-03	-1.84E-09
-18	-1.92E-09	-4.98E-09	-3.87E-04	-1.37E-09	-6.42E-04	-1.61E-09	-1.00E-03	-1.85E-09	-1.00E-03	-1.70E-09
-16	-1.64E-09	-2.70E-09	-6.74E-06	-1.44E-09	-9.38E-06	-1.47E-09	-1.00E-03	-1.76E-09	-1.00E-03	-1.41E-09
-14	-1.38E-09	-1.72E-09	-8.50E-09	-1.25E-09	-1.07E-08	-1.40E-09	-8.45E-04	-1.52E-09	-8.13E-04	-1.37E-09
-12	-1.40E-09	-1.48E-09	-3.66E-09	-1.12E-09	-4.28E-09	-1.31E-09	-4.59E-04	-1.56E-09	-4.89E-04	-1.32E-09
-10	-1.36E-09	-1.10E-09	-1.70E-09	-9.86E-10	-1.57E-09	-1.19E-09	-2.60E-04	-1.47E-09	-1.67E-04	-1.28E-09
-8	-1.22E-09	-1.11E-09	-1.28E-09	-9.25E-10	-1.09E-09	-1.01E-09	-1.15E-04	-1.13E-09	-5.85E-05	-8.47E-10
-6	-1.06E-09	-1.01E-09	-7.62E-10	-7.79E-10	-8.22E-10	-1.05E-09	-4.00E-05	-1.05E-09	-7.47E-06	-7.67E-10
-4	-7.94E-10	-6.85E-10	-5.99E-10	-6.36E-10	-6.71E-10	-9.81E-10	-4.49E-06	-9.64E-10	-5.14E-07	-7.73E-10
-2	-7.45E-10	-8.36E-10	-7.60E-10	-6.18E-10	-6.67E-10	-1.09E-09	-1.48E-07	-1.16E-09	-4.50E-08	-7.31E-10
0	-7.14E-10	-8.97E-10	-6.32E-10	-7.52E-10	-6.56E-10	-1.57E-09	-2.58E-10	-1.72E-09	-4.60E-10	-5.30E-10
2	1.03E-09	9.98E-10	3.06E-08	9.77E-10	2.14E-08	9.63E-10	9.23E-08	7.67E-10	1.71E-07	6.69E-10
4	7.59E-10	6.69E-10	2.81E-05	7.24E-10	3.02E-06	7.97E-10	4.91E-06	7.69E-10	5.47E-06	5.63E-10
6	6.25E-10	7.78E-10	2.83E-04	8.31E-10	1.66E-04	7.20E-10	2.72E-04	5.05E-10	2.63E-04	5.29E-10
8	1.01E-09	9.01E-10	8.06E-04	8.68E-10	1.00E-03	8.17E-10	1.00E-03	6.31E-10	1.00E-03	7.07E-10
10	8.78E-10	9.12E-10	1.00E-03	8.80E-10	1.00E-03	8.43E-10	1.00E-03	7.53E-10	1.00E-03	8.88E-10
12	1.04E-09	1.17E-09	1.00E-03	9.58E-10	1.00E-03	9.07E-10	1.00E-03	6.14E-10	1.00E-03	7.30E-10
14	1.07E-09	1.61E-09	1.00E-03	9.50E-10	1.00E-03	1.03E-09	1.00E-03	9.07E-10	1.00E-03	6.50E-10
16	1.02E-09	2.81E-09	1.00E-03	1.24E-09	1.00E-03	1.12E-09	1.00E-03	9.33E-10	1.00E-03	8.92E-10
18	1.33E-09	5.23E-09	1.00E-03	1.22E-09	1.00E-03	1.25E-09	1.00E-03	8.90E-10	1.00E-03	1.03E-09
20	1.74E-09	1.29E-08	1.00E-03	1.22E-09	1.00E-03	1.36E-09	1.00E-03	1.22E-09	1.00E-03	1.20E-09

Run # DUT S/N Date	85 21 1/23/2011	86 21 1/23/2011	pre-87 17 1/23/2011	87 17 1/23/2011	pre-88 18 1/23/2011	88 18 1/23/2011	90 22 1/24/2011	91 22 1/24/2011
Vgs (V):	Ids (A):							
0	-1.60E-09	-1.55E-09	-2.76E-09	-4.98E-10	-9.45E-10	-9.54E-10	-1.47E-09	-9.33E-10
-2	-9.27E-10	-1.87E-08	-2.93E-09	-1.32E-07	-1.00E-09	-4.17E-07	-1.09E-09	-1.22E-08
-4	-1.24E-09	-4.95E-07	-2.39E-09	-1.73E-06	-9.31E-10	-3.24E-06	-1.03E-09	-1.98E-07
-6	-1.39E-09	-5.27E-06	-2.28E-09	-1.93E-05	-1.17E-09	-1.84E-05	-1.17E-09	-2.70E-06
-8	-1.58E-09	-2.72E-05	-2.33E-09	-8.76E-05	-1.28E-09	-6.17E-05	-1.22E-09	-1.99E-05
-10	-2.01E-09	-1.26E-04	-2.73E-09	-2.82E-04	-1.58E-09	-1.70E-04	-1.17E-09	-9.67E-05
-12	-1.65E-09	-8.56E-04	-3.10E-09	-6.12E-04	-1.52E-09	-8.04E-04	-1.57E-09	-5.24E-04
-14	-1.47E-09	-1.00E-03	-3.72E-09	-7.18E-04	-1.54E-09	-1.00E-03	-1.53E-09	-1.00E-03
-16	-1.96E-09	-1.00E-03	-3.25E-09	-1.00E-03	-1.59E-09	-1.00E-03	-1.63E-09	-1.00E-03
-18	-1.82E-09	-1.00E-03	-2.47E-09	-1.00E-03	-1.87E-09	-1.00E-03	-1.51E-09	-1.00E-03
-20	-2.06E-09	-1.00E-03	-3.52E-09	-1.00E-03	-1.89E-09	-1.00E-03	-1.77E-09	-1.00E-03
2	1.18E-09	6.02E-06	-1.19E-09	2.26E-05	8.61E-10	1.61E-06	8.24E-10	2.04E-08
4	5.16E-10	1.48E-05	-1.47E-09	1.36E-04	5.95E-10	4.98E-06	6.44E-10	4.18E-07
6	4.75E-10	2.01E-04	-1.63E-09	5.83E-04	5.60E-10	4.54E-05	5.72E-10	1.71E-05
8	5.66E-10	1.00E-03	-7.05E-10	1.00E-03	7.67E-10	1.00E-03	7.53E-10	1.89E-04
10	5.48E-10	1.00E-03	-1.10E-09	1.00E-03	7.76E-10	1.00E-03	6.88E-10	1.00E-03
12	1.08E-09	1.00E-03	-9.62E-10	1.00E-03	7.92E-10	1.00E-03	7.80E-10	1.00E-03
14	8.26E-10	1.00E-03	-1.33E-09	1.00E-03	1.02E-09	1.00E-03	1.08E-09	1.00E-03
16	6.86E-10	1.00E-03	-1.32E-09	1.00E-03	8.54E-10	1.00E-03	1.04E-09	1.00E-03
18	1.10E-09	1.00E-03	6.39E-10	1.00E-03	1.43E-09	1.00E-03	1.14E-09	1.00E-03
20	9.23E-10	1.00E-03	-6.04E-10	1.00E-03	1.35E-09	1.00E-03	1.24E-09	1.00E-03

## Appendix E

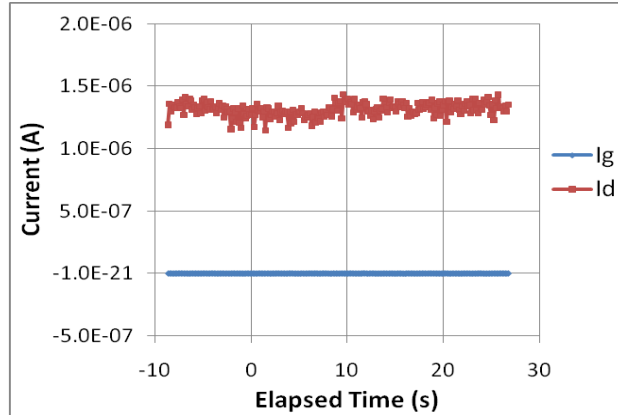


Fig. E1. SMU current measurements of DUT 1 during run 3 with Ag. This sample failed immediately after the run during the post-irradiation gate stress test (see Appendix D).  
 $V_{gs} = 0$  V,  $V_{ds} = -170$  V.

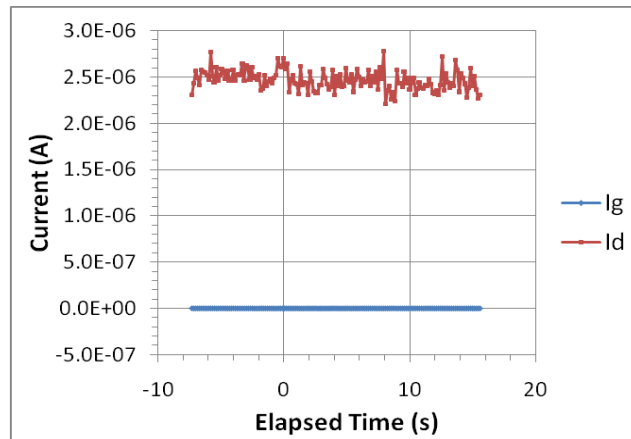


Fig. E2. Another example of SMU current measurements for an Ag run after which failure occurred during the PIGS test.  
 $V_{gs} = 0$  V,  $V_{ds} = -165$  V. DUT 7, run 13.

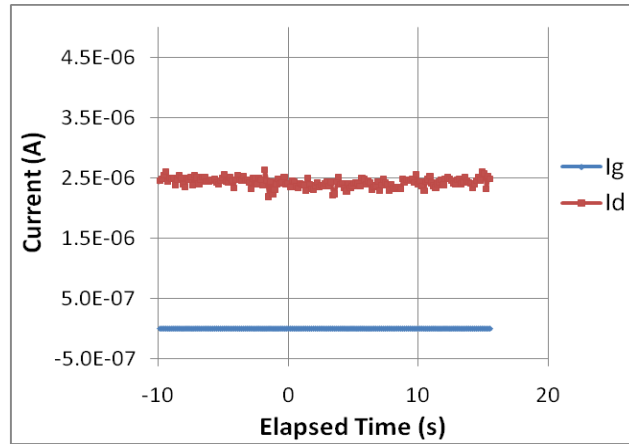


Fig. E3. Example of SMU current measurements during an Ag run for which no failure occurred during the following PIGS test.  
 $V_{gs} = 0$  V,  $V_{ds} = -170$  V. DUT 4, run 6.

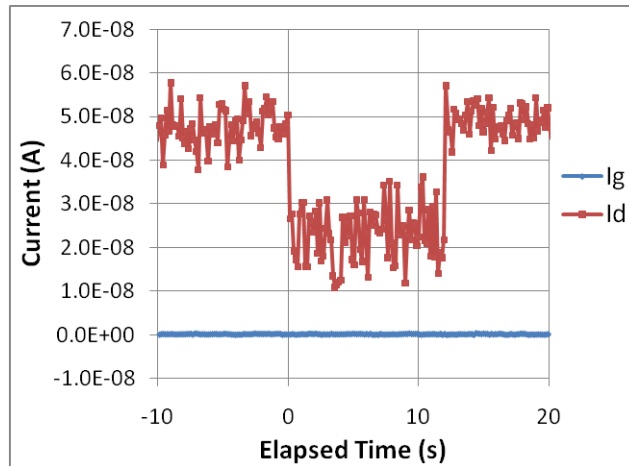


Fig. E4. Example of SMU current measurements during an Ag run in which the noise level on  $I_d$  was low enough to detect the excess drain current resulting from the charge ionized by the beam.  
 $V_{gs} = 5$  V,  $V_{ds} = -100$  V. DUT 11, run 19.

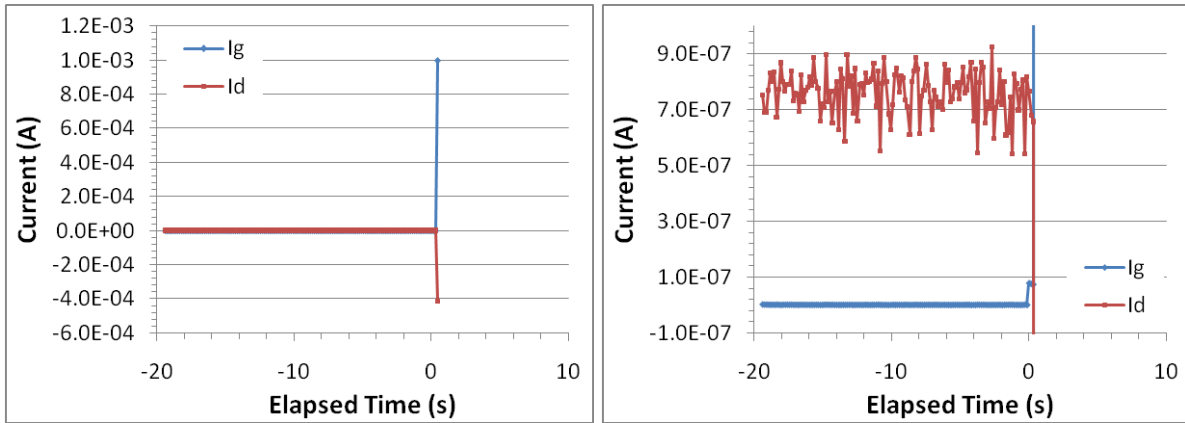


Fig. E5. SMU current measurements showing device failure during Ag beam run. Left: Gate current reaches the SMU current limit of 1 mA. Right: Smaller current scale reveals that the gate suffered a small rupture prior to the large rupture.  $V_{gs} = 10$  V,  $V_{ds} = -40$  V. DUT 10, run 40.

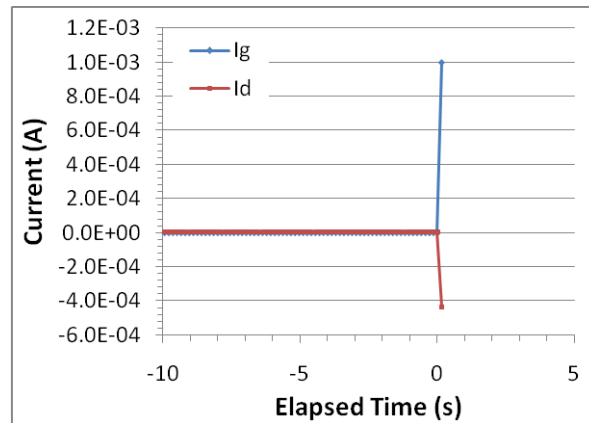


Fig. E6. SMU current measurements during Ag beam run showing DUT failure immediately after the beam was turned on.  $V_{gs} = 10$  V,  $V_{ds} = -40$  V. DUT 15, run 43.

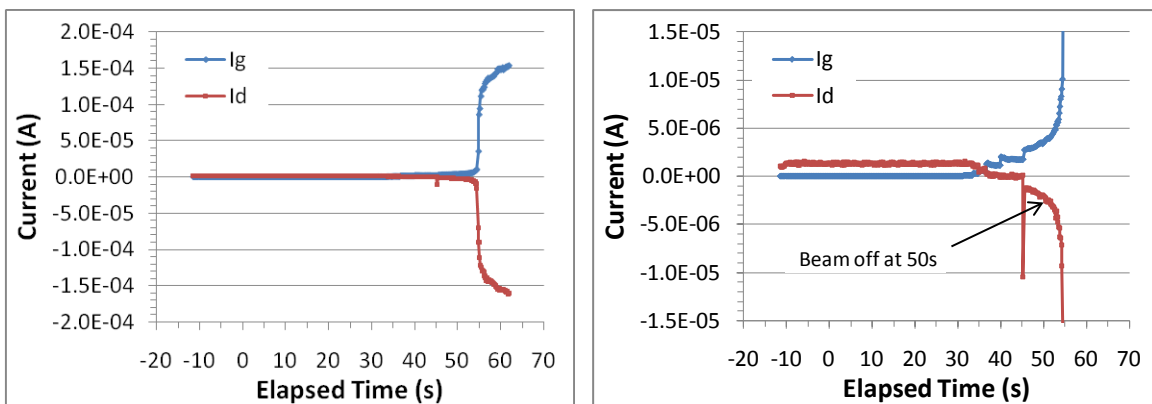


Fig. E7. SMU current measurements during Kr beam run. The currents continued to increase after the beam was shuttered (DUT remained under bias).  $V_{gs} = 10$  V,  $V_{ds} = -200$  V. DUT 21, run 86.

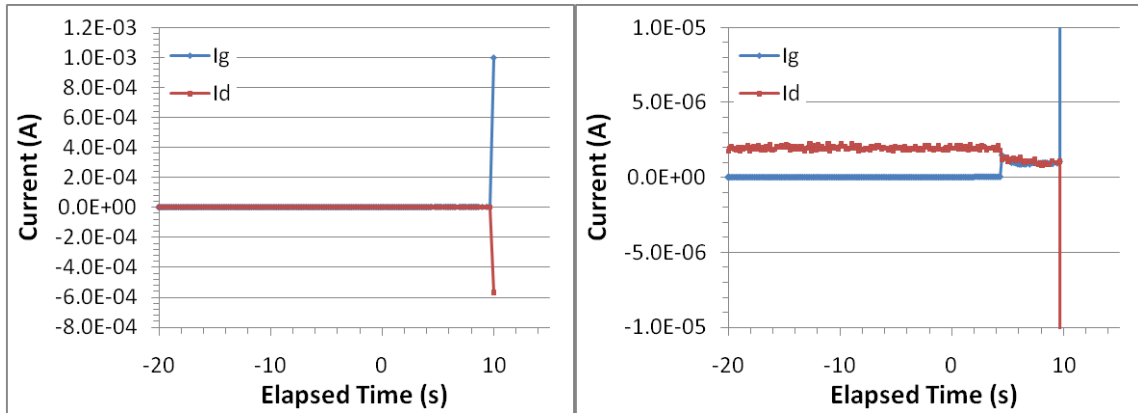


Fig. E8. SMU current measurements during Kr beam run. Left: Gate current reaches the SMU current limit of 1 mA. Right: Smaller current scale reveals that the gate suffered a small rupture prior to the large rupture.  $V_{gs} = 10 \text{ V}$ ,  $V_{ds} = -180 \text{ V}$ . DUT 17, run 87.

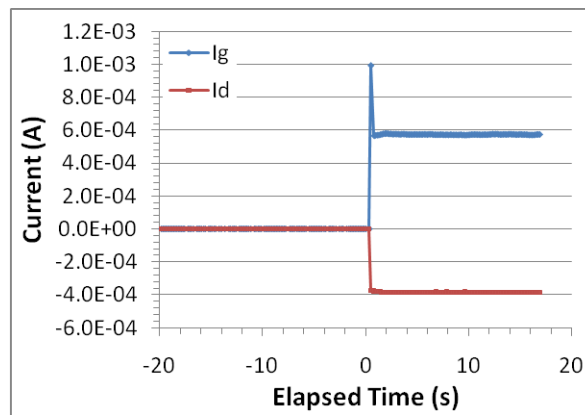


Fig. E9. SMU current measurements during Kr beam run showing gate rupture immediately upon irradiation. The gate current stabilized under bias, but returned to the SMU current limit of 1 mA during the PIGS test following this beam run.  $V_{gs} = 10 \text{ V}$ ,  $V_{ds} = -150 \text{ V}$ . DUT 18, run 88.

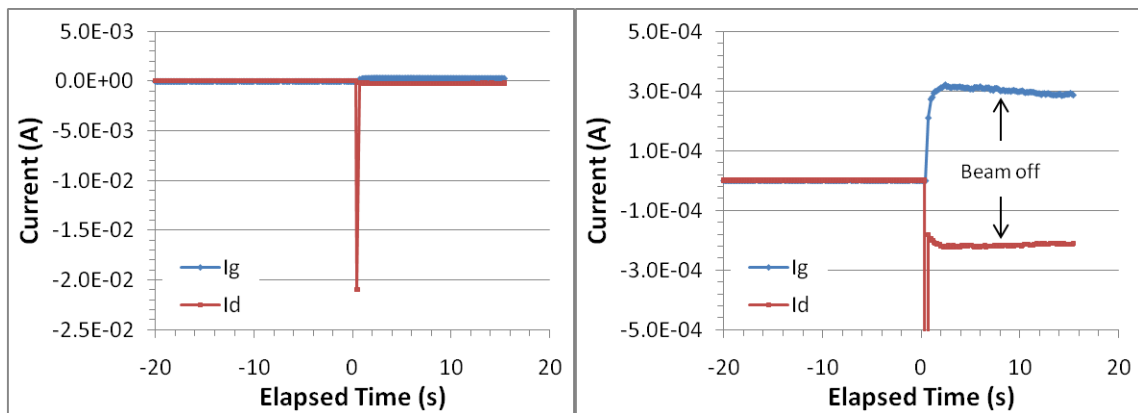


Fig. E10. SMU current measurements during Kr beam run.  $V_{gs} = 10 \text{ V}$ ,  $V_{ds} = -140 \text{ V}$ . DUT 22, run 91.

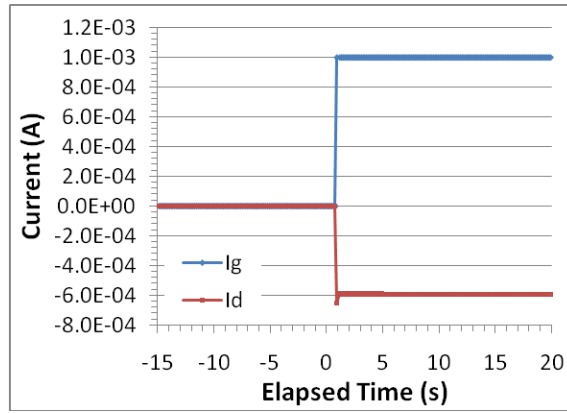


Fig. E11. SMU current measurements during Kr beam run. In this case, the gate current remained at the 1 mA supply current limit after the gate ruptured.  $V_{gs} = 10\text{ V}$ ,  $V_{ds} = -125\text{ V}$ . DUT 41, run 74.

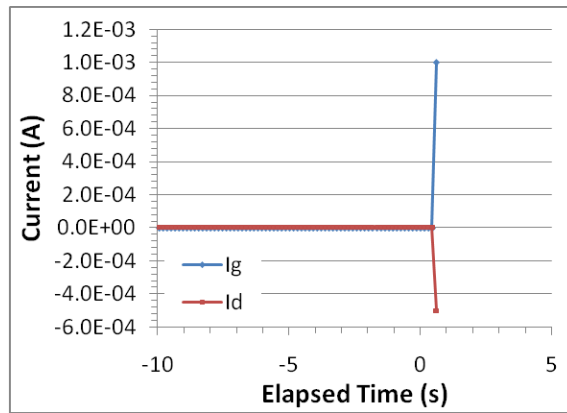


Fig. E12. SMU current measurements during Kr beam run.  $V_{gs} = 10\text{ V}$ ,  $V_{ds} = -110\text{ V}$ . DUT 42, run 75.